

Effect of atomic oxygen on the initial growth mode in thin epitaxial cuprate films

T. Frey, C. C. Chi, C. C. Tsuei, T. Shaw, and F. Bozso

IBM Research Division, Thomas J. Watson Research Center, Yorktown Heights, New York 10598

(Received 11 June 1993)

The basic growth mode of a thin epitaxial cuprate film ($< 200 \text{ \AA}$) on a given substrate depends sensitively on the balance between various thermodynamic and kinetic factors related to the high- T_c phase formation and the surface microstructure at the growth front of the deposited film. Under the standard optimized growth conditions for high-quality epitaxial films, the deposition of a $\text{YBa}_2\text{Cu}_3\text{O}_{7-\delta}$ film on an atomically smooth (110) SrTiO_3 substrate, for example, is characterized by a strong damping in the reflection high-energy electron diffraction (RHEED) oscillation suggesting a predominant island growth mode. We have demonstrated that with an atomic oxygen and the technique of RHEED-controlled growth interruption it is possible to minimize surface roughness and to fabricate unit-cell smooth $\text{YBa}_2\text{Cu}_3\text{O}_{7-\delta}$ films over a large area ($\sim 0.5 \text{ cm} \times 1 \text{ cm}$). The results of this study suggest that two-dimensional layer growth can be induced by the combined use of atomic oxygen and growth conditions, such as low deposition rate, low oxygen partial pressure ($< 2 \text{ mTorr}$), that produce low supersaturation at the growth front.

I. INTRODUCTION

A better understanding of the basic processes and mechanisms in the epitaxial deposition of high- T_c cuprate films, especially during the initial stages of the film growth, is important for the study of superconductivity in ultrathin cuprate films. For example, in order to make a definitive statement about the superconducting properties of a nominally one-unit-cell (uc)-thick cuprate layer (such as in single-layer or multilayer superlattice configurations), one should be quite sure that the roughness at the layer surface or interface does not exceed one uc in magnitude over a large area. Otherwise, the observed transport and magnetic properties may reflect mostly those of much thicker films with the effects due to granularity and percolation. Furthermore, the capability of growing epitaxial films with atomic smoothness is obviously crucial in the synthesis of new layered superconductors via atomic-scale layer-by-layer materials engineering.

In recent years, significant progress has been made in understanding the growth kinetics and mechanisms in the growth of epitaxial cuprate films.¹⁻⁷ One remaining unsolved problem is the origin of the observed intensity oscillations in reflection high-energy electron diffraction (RHEED) during the process of film deposition. Based on their RHEED results, Terashima *et al.*¹ claimed success in achieving uc-by-uc layer growth of $\text{YBa}_2\text{Cu}_3\text{O}_7$ (YBCO) epitaxial films on (100) SrTiO_3 substrates. On the other hand, Chandrasekhar *et al.*² interpreted their RHEED oscillations data as arising from changing surface step densities and suggested that the basic film growth mode is that of island growth instead of the cyclic layer uc-by-layer growth. The discrepancy between these two different view points on growth modes may stem from the difference in the interpretation of the RHEED data, but it is also possible that it is due to some subtle difference in sample fabrication conditions which may de-

pend on the film deposition system used. Ideally, to gain more insight into these issues, a complete systematic study of the effects of various film preparation conditions on the growth mode is needed. However, in view of the vast growth parameter space, one should not expect a unique set of growth conditions for a specific growth mode in the epitaxy of cuprates.

In this work, we do not intend to settle these controversial issues, rather we will concentrate in manipulating a few selected growth parameters to explore the feasibility of uc scale layer-by-layer epitaxy in cuprates, using the technique of RHEED-controlled laser-molecular beam epitaxy (MBE).⁷ In particular, we emphasize the use of atomic oxygen for promoting the growth of *large area* uc smooth epitaxial cuprate films.

II. EXPERIMENTAL DESCRIPTION

The basic film deposition apparatus used in this work is a computer-controlled laser-MBE system (Fig. 1) equipped with a differentially pumped *in situ* RHEED system and an atomic oxygen source. A similar laser-MBE system using ozone or other oxidants has been employed by Kawai⁸ and Gupta⁵ in their work on growing various epitaxial cuprate films.

The RHEED system is used for *in situ* monitoring of film growth as well as film thickness. A 20 KeV electron beam is focused to the substrate surface with an angle of incidence of 1.5° to 2.5° along the [100] or [110] direction of the substrate. The incidence angle was determined from the distance of the direct beam and the specular reflection image spot on the phosphor screen. For the ideal operation of RHEED during film growth, the basic chamber background pressure (P_0) should be kept below 10^{-4} Torr. With the constraint of base chamber pressure and the necessity of satisfying the oxygen activity requirement for kinetic and thermodynamic stability of the high- T_c phase,⁴ the use of a differential pump and an

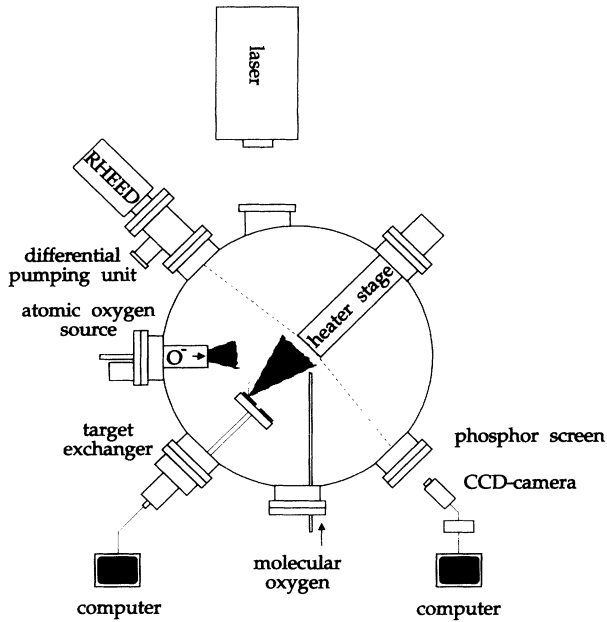


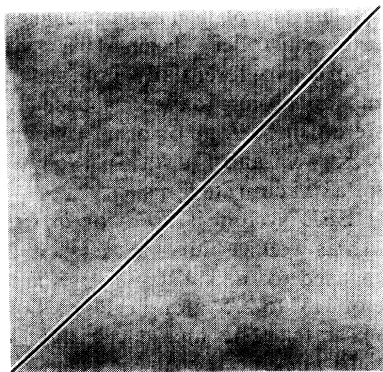
FIG. 1. Schematic diagram of the computer-controlled laser-MBE system.

atomic oxygen source is essential. The atomic oxygen source used in this work is a 500 W rf plasma generator which produces a high flux of very reactive atomic oxygen. The flux of atomic oxygen was estimated to be $2-5 \times 10^{16}$ atomic oxygen $\text{cm}^{-2} \text{s}^{-1}$ by using a mass spectrometer. The distance between the atomic oxygen source and the substrate is 8 cm and the oxygen beam is directed at an angle of 60° to the substrate surface. To assure full oxidation of all ablated materials arriving at the substrate with each laser pulse, an additional continuous

local spray of molecular oxygen is provided through a small nozzle (5 mm diam) positioned as close as 1 cm in front of the substrate. The combined use of atomic and molecular oxygen results in an overall background pressure in the deposition chamber which is about 10^{-3} Torr. This pressure does not degrade the performance of the RHEED system used in this work.

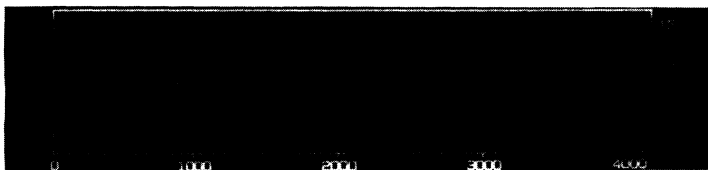
As a template for epitaxial film growth, the substrate and its surface condition play extremely important roles in determining the structure and surface morphology of the deposited film, especially during the initial stages of growth. In this work, we carefully selected high-quality optically polished (100)-oriented SrTiO_3 substrates with a miscut angle of less than 1° and an average surface smoothness less than 8 \AA over an area of $\sim 1 \text{ cm} \times 1 \text{ cm}$. A typical atomic force microscope (AFM) image of one of the substrates and its typical line scans are shown in Figs. 2(a) and 2(b). The AFM used in this work has the z -direction resolution of 0.1–0.2 nm and an x and y -scan range of $15 \mu\text{m}$. As shown in these figures, the surface of the SrTiO_3 substrates used in this study are, indeed, atomic-scale smooth. The smoothness can further be improved by homoepitaxial deposition of SrTiO_3 on SrTiO_3 . The RHEED pattern shown in Fig. 3 is from a (100) SrTiO_3 substrate after heating for 5 min in O_2 (200 mTorr) at a temperature of $\approx 850^\circ\text{C}$ followed by a deposition of a 70 \AA buffer layer of SrTiO_3 at 750°C . The clear, streaky RHEED pattern along with the development of Kikuchi lines suggest that a very smooth and well-ordered surface is formed after the deposition.

The cuprate films were deposited using a KrF (248 nm) excimer laser with a pulse repetition rate of 2–5 Hz and a fluence of $\sim 1.5-2 \text{ J/cm}^2$ at the target. A well-sintered high-density cuprate target was used for ablation. A computer-controlled target exchanger allows any predetermined sequence of four targets for *in situ* sequen-



(a)

FIG. 2. (a) AFM image ($3 \mu\text{m} \times 3 \mu\text{m}$) for a typical (100) SrTiO_3 substrate used in this study. (b) Typical line scan of the SrTiO_3 substrate with a corrugation of less than 5 \AA over $4.2 \mu\text{m}$. (Both vertical and horizontal scales are in nm.)



(b)

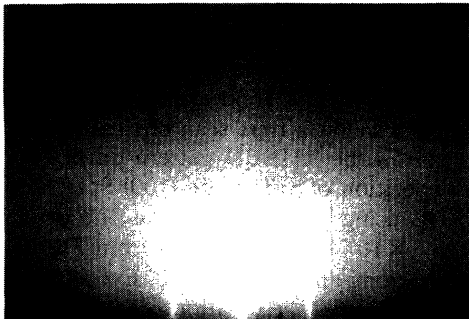


FIG. 3. RHEED patterns of the (100) SrTiO₃ along (100) substrate azimuth after homoepitaxial growth of a 18 monolayer (ML) buffer. ($T_s = 750^\circ\text{C}$, using atomic oxygen $P_0 \sim 10^{-4}$ Torr, beam energy 20 KeV.)

tial film deposition. The substrate-target distance was varied between 5 cm to 10 cm. For film homogeneity, it was found that this distance should be 8 cm or larger.

III. RESULTS AND DISCUSSION

The RHEED pattern and the intensity of the specular beam were constantly monitored during the entire process of film deposition in order to measure the film thick-

ness *in situ*, as well as for controlling the μc scale layer-by-layer growth. It is, therefore, important to describe how the RHEED pattern, especially its temporal dependence, is expected to vary with the evolution of surface structure and morphology at the growth front of the deposited film. In the literature, there are many examples of using RHEED information for achieving the epitaxy of semiconductors⁹ and more recently, for high- T_c superconductors.^{1,2,5-7} Various models⁹⁻¹² have been proposed to understand RHEED data, especially the RHEED oscillations in terms of the time evolution of the step density and/or the terrace areas on the film surface. On the other hand, it is well established that experimental factors such as the RHEED diffraction condition and film deposition parameters can significantly affect the RHEED signal. Without getting involved in these details, we have adopted what is shown in Fig. 4 as a general guide for understanding the RHEED data and for *in situ* monitoring and controlling our film growth process. In Fig. 4, a schematic description of the temporal evolution of the RHEED patterns for various basic modes of thin-film growth is given.

Figure 4(a) shows layer-by-layer growth (Frank-van der Merwe mode). Strictly speaking, layer-by-layer growth is a self-terminating cyclic deposition process: i.e., the growth of a second atomic layer will not be ini-

Basic Growth Modes of Epitaxial Thin Films

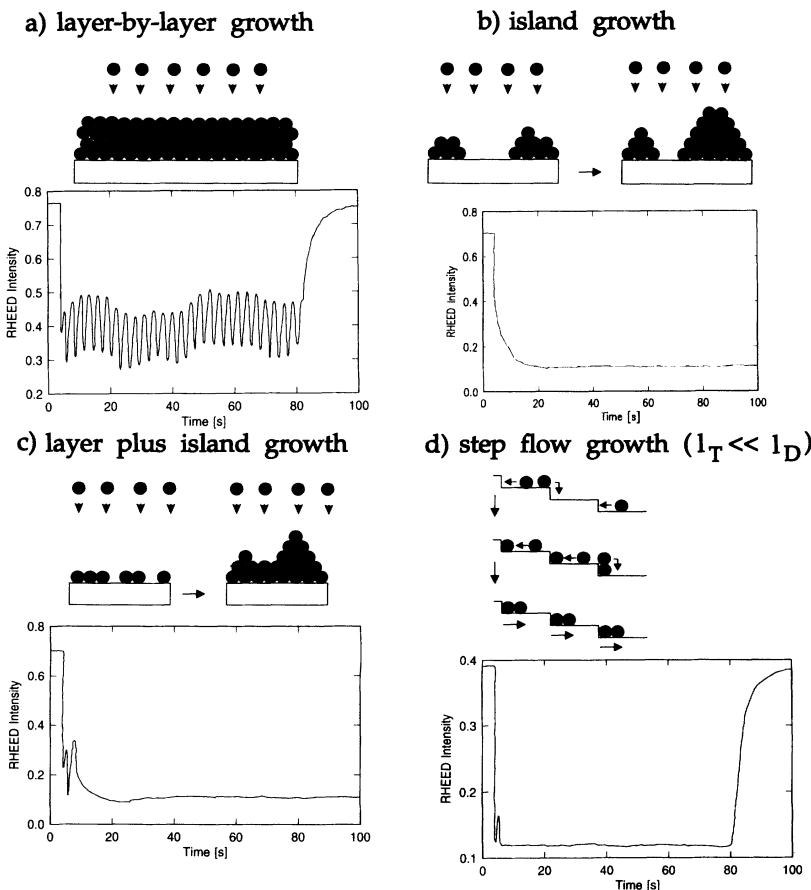


FIG. 4. Schematic description of the various thin-film growth modes and the corresponding time scans of the RHEED specular beam intensities during film growth: (a) layer-by-layer growth, (b) island growth, (c) layer plus island growth, (d) step-flow growth.

tiated until the first layer is fully covered. The RHEED specular beam intensity should oscillate periodically in time without significant damping in its magnitude. After the deposition stops, the RHEED intensity should fully recover.

Figure 4(b) shows island growth (Volmer-Weber mode). Under certain experimental growth conditions (low substrate temperature T_s , high particle flux, and high background pressure P_0), a high supersaturation at the substrate may be produced. This situation favors island growth. The step density varies nonperiodically and multiple diffuse scattering from various steps may dominate the RHEED electron-scattering process which leads to a sharp drop in RHEED intensity and no oscillations in the reflected beam. Furthermore, electron transmission through three-dimensional (3D) island surface features will give rise to spotty RHEED patterns.

Figure 4(c) shows layer-by-layer plus island growth (Stranski-Krastanov mode). Under certain thermodynamic and kinetic conditions,⁴ strain-driven pseudomorphic growth will prevail in the initial deposition of a few atomic layers. However, this situation can be altered if the particle flux is too high or the surface mobility is no longer high enough to support two-dimensional (2D) growth. In this case, very few RHEED oscillations should be observed and no significant recovery is to be expected.

Figure 4(d) shows the step-flow growth mode. If the substrate surface terrace length l_T is much smaller than the surface diffusion length l_D , surface steps on the substrate surface represent energetically favorable sites for nucleation.⁴ The step density, after the initial film growth, will reach a steady state, giving rise to a constant RHEED intensity as a function of time. Strong recovery should be observed when the deposition is terminated.

In reality, true layer-by-layer growth is difficult to achieve. Using standard growth conditions, for example, 200 mTorr O_2 , $T_s \approx 750^\circ C$, for making high-quality epitaxial cuprate films, one usually produces epitaxial films characterized by dislocation-mediated spiral growth and a very rough surface.^{13,14} In this study we adopt the so-called growth-interruption technique for growing smooth cuprate film over a large area. The validity and relevance of this approach for the epitaxy in cuprates can be tested by studying the surface morphology using AFM and/or (scanning tunneling microscope) STM, and by checking the consistency of various film thickness measurements using the method of counting RHEED oscillations and other techniques, such as small-angle x-ray diffraction (XRD) and cross sectional TEM. In this spirit, the results of RHEED and AFM measurements on various thin epitaxial cuprate films grown on the (100) $SrTiO_3$ substrates are presented in the following sections. The effect of using atomic oxygen during the film growth on the surface morphology of the deposited films is emphasized.

A. Homoepitaxial growth of $SrTiO_3$ on $SrTiO_3$

To achieve layer-by-layer epitaxial film growth [Fig. 4(a)], it is of the utmost importance that the substrate is

atomically smooth over a large area and that the lattice mismatch between the substrate and deposited film is as small as possible. The homoepitaxial growth of a $SrTiO_3$ film on (100) $SrTiO_3$ is a good example to illustrate this point. Figure 5 shows a time scan of the intensity of the specular beam in the RHEED pattern during homoepitaxial film deposition of $SrTiO_3$ on (100) $SrTiO_3$ substrate at $T_s = 750^\circ C$ using atomic oxygen as the primary oxidant at $P_0 \sim 2 \times 10^{-3}$ Torr. As seen from Fig. 5, the oscillations are strong and well defined. Even after the 18th period, the RHEED oscillations are only slightly damped. After the film growth is terminated, a strong recovery of the RHEED intensity is always observed. It should be mentioned that to ensure an atomically smooth surface of the deposited film, it is best to stop film growth when the RHEED intensity is at the peak (as shown in Fig. 5), when the film coverage of the topmost layer is presumably complete. Also, as shown in the Fig. 5, the intensity after deposition is higher than the starting value, suggesting that the surface smoothness has been improved as a result of the homoepitaxy. The RHEED patterns after the $SrTiO_3$ deposition are sharp and streaky and the development of Kikuchi lines, for example, as shown in Fig. 3, clearly demonstrates that the surface imperfections on the substrate have been "repaired." It was found that the preparation of an atomically smooth (100) $SrTiO_3$ substrate surface is crucial in determining the quality and growth mode of the high- T_c cuprate films to be deposited. In short, the results presented above suggest that the homoepitaxy of $SrTiO_3$ on $SrTiO_3$ can probably be described by a layer-by-layer growth mode.

B. Heteroepitaxial growth of high- T_c cuprates on $SrTiO_3$

When a film-substrate lattice mismatch does exist as in the cases of heteroepitaxial growth of high- T_c cuprates on $SrTiO_3$, the true layer-by-layer growth is not possible but can be approximated by judiciously selecting a set of growth parameters and using the *in situ* RHEED-controlled growth technique along with the use of a high flux of atomic oxygen.

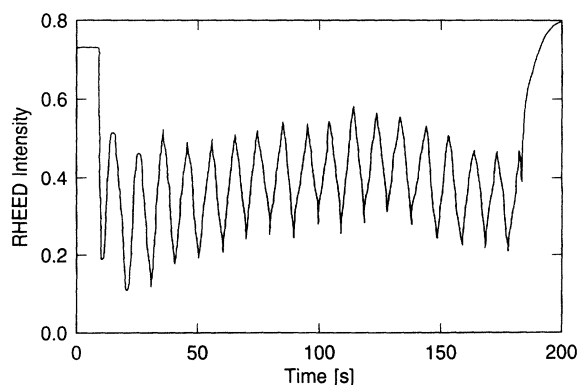


FIG. 5. RHEED specular beam intensity oscillations for homoepitaxial growth of $SrTiO_3$ on (100) $SrTiO_3$ substrate taken along the (100) substrate azimuth. ($T_s = 750^\circ C$, beam energy 20 KeV.)

The most important growth parameters for growing high-quality cuprate films are found to be the oxygen partial pressure, oxygen potency, substrate temperature (T_s), and growth rate.⁷ In general, the substrate temperature should be high enough to ensure adequate atomistic surface mobility at the film growth front and also, more importantly, to satisfy the thermodynamic and kinetic requirements for the high- T_c phase stability under the experimental oxygen ambient condition. However, the substrate temperature should be low enough to prevent interlayer diffusion and film-substrate interaction from occurring. In the case of YBCO on (100) SrTiO₃, too low a substrate temperature ($T_s = 710^\circ\text{C}$, $P_0 = 5$ mTorr, for example), results in very rough mixed c - and a -axis-oriented YBCO films as reported previously.⁷ In this case, the basic growth mode is probably dominated by the process of island growth and coalescence [as schematically depicted in Fig. 4(c)].

With a similar substrate temperature, another cuprate system can exhibit a very different growth behavior. A typical time scan of the specular RHEED beam intensity for a La_{1.85}Sr_{0.15}CuO₄ (LSCO) film deposition at $T_s = 730^\circ\text{C}$, using the optimized combination of molecular and atomic oxygen at $P_0 \sim 2 \times 10^{-3}$ Torr, is shown in Fig. 6. Typically, as many as 30 strong and only slightly damped RHEED oscillations can be recorded before film deposition has to be interrupted to give the surface time for recovery and self-smoothing. The corresponding RHEED pattern of a 2000 Å-thick film growth with the atomic oxygen-enhanced growth-interruption technique, as shown in Fig. 7(b) is sharp and streaky, indicating a rather smooth film surface. The film surface shows large terraces with typical step heights of ~ 6.5 and ~ 13 Å, as measured by AFM [Fig. 7(a)]. The film is smooth on a unit-cell scale over the measured area of $2 \mu\text{m} \times 2 \mu\text{m}$. The thickness values of various measurements (counting oscillations and small-angle x-ray data) are consistent with each other within $\sim 5\%$. A detailed account of the growth process in this cuprate system will be presented elsewhere.

On the other hand, to sustain the RHEED oscillations

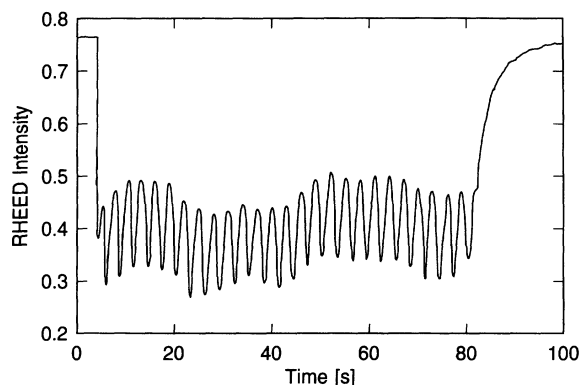
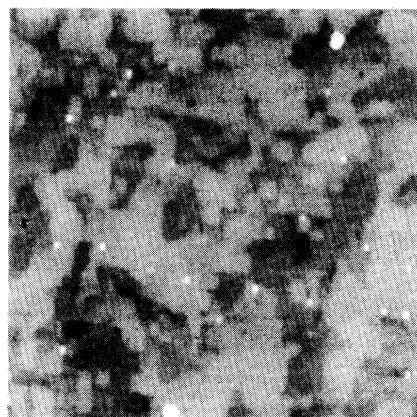
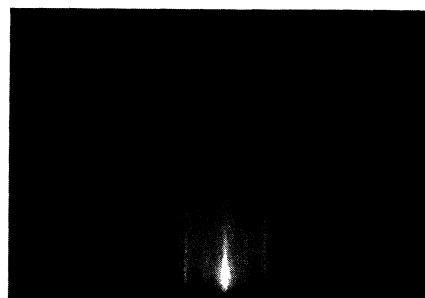


FIG. 6. RHEED specular beam intensity oscillations [along (100) azimuth] during a sequence of heteroepitaxial growth of La_{1.85}Sr_{0.15}CuO₄ on (100) SrTiO₃ substrate. Beam energy 20 KeV, $T_s = 730^\circ\text{C}$ using a combination of molecular and atomic oxygen at $P_0 \sim 2 \times 10^{-3}$ Torr.



(a)



(b)

FIG. 7. (a) AFM image ($2 \mu\text{m} \times 2 \mu\text{m}$) of a ~ 2000 Å-thick LSCO film. (b) RHEED patterns along the (100) azimuth of a 2000 Å-thick LSCO film at $T_s = 730^\circ\text{C}$. Beam energy 20 KeV.

without severe damping in the intensity and oscillation amplitude is much more difficult to achieve in the YBCO (100) SrTiO₃ system. A time scan of the RHEED pattern recorded during a typical deposition of a three-unit-cell-thick YBCO film on a (100) SrTiO₃ substrate at $T_s = 740^\circ\text{C}$ is shown in Fig. 8. All other growth conditions were optimized, including using atomic oxygen and

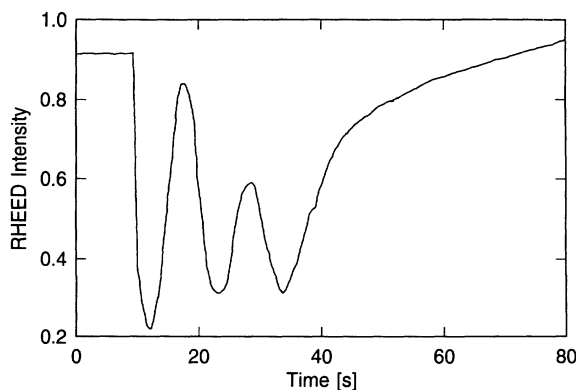


FIG. 8. Typical RHEED intensity oscillations during the initial growth of 3 uc YBCO on a 5-uc-thick PBCO buffer using a (100) SrTiO₃ substrate.

Growth of unit-cell smooth films: using RHEED-controlled growth interruption technique

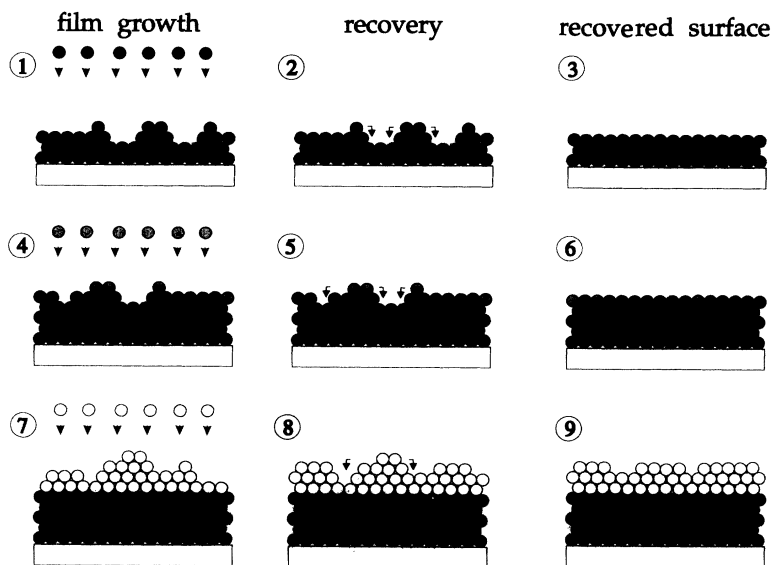


FIG. 9. Schematic diagram for the basic process of self-smoothing and self-substrate epitaxial growth. (Corresponding RHEED intensity oscillations are shown in Fig. 10.)

a smooth (100) SrTiO_3 substrate with a five-uc-thick $\text{PrBa}_2\text{Cu}_3\text{O}_{(7-\delta)}$ (PBCO) buffer layer. In spite of all these efforts, the RHEED oscillation amplitude is damped severely after only two to three periods, suggesting an island growth or step-flow mode.

In the following, RHEED data and AFM results on the YBCO films grown on SrTiO_3 will be used to emphasize that a combined use of atomic oxygen as the primary oxidant and the technique of growth interruption can indeed effectively achieve unit-cell smooth high- T_c YBCO epitaxial films over large areas ($\sim 0.5 \text{ cm} \times 1 \text{ cm}$). The basic technique of using growth interruption for better epitaxy in semiconductors⁹ and for high- T_c cuprates¹ has already been reported. The strong RHEED intensity recovery after the termination of the YBCO film deposition (Fig. 8) indicates that there is a strong surface smoothing at the film surface and that the freshly grown epitaxial YBCO film is ready for more epitaxial growth $\sim 20 \text{ s}$ after deposition is interrupted.

The basic idea of using atomic oxygen as an oxidant is to assure that the constrain on ambient chamber pressure imposed by the RHEED operation requirement does not jeopardize the stability of the high- T_c YBCO phase. It is suggested in the literature, that a higher potency of the oxidant can lower the required substrate temperature and oxygen partial pressure for phase stability.¹⁵⁻¹⁷ As a result of using atomic oxygen, the supersaturation is reduced and the two-dimensional layer-by-layer growth is favored over the island growth process.

Figure 9 shows schematically the basic process of self-smoothing and self-substrate epitaxial film growth using the growth-interruption approach described earlier. Steps 1-9 represent three film deposition cycles which stop only at a time corresponding to a local maximum of

RHEED intensity and restart when the RHEED intensity has recovered to about its starting value. The time scan of the RHEED intensity in Fig. 10 shows three such growth cycles of YBCO film deposition on (100) SrTiO_3 substrate: a three-uc-thick layer was deposited during the first and the third cycles, while a two-uc-thick layer was grown in the second cycle, a situation depicted schematically in Fig. 9. The growth rate was changed (by using a different layer repetition rate) after deposition of the first three uc. Time periods of the RHEED oscillations were measured to be inversely proportional to the growth rate. The observed recovery of the specular RHEED beam intensity after film growth is interrupted, may be due to an increase in the mean terrace width of

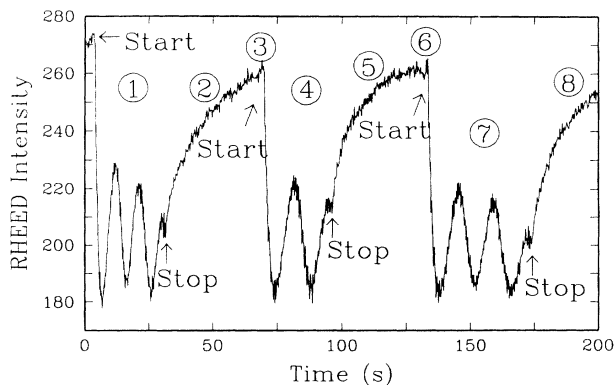


FIG. 10. A time scan of the specular RHEED beam intensity during deposition of a YBCO film on (100) SrTiO_3 with a PBCO buffer using the growth-interruption technique. Growth rate was changed after deposition of the first three layers.

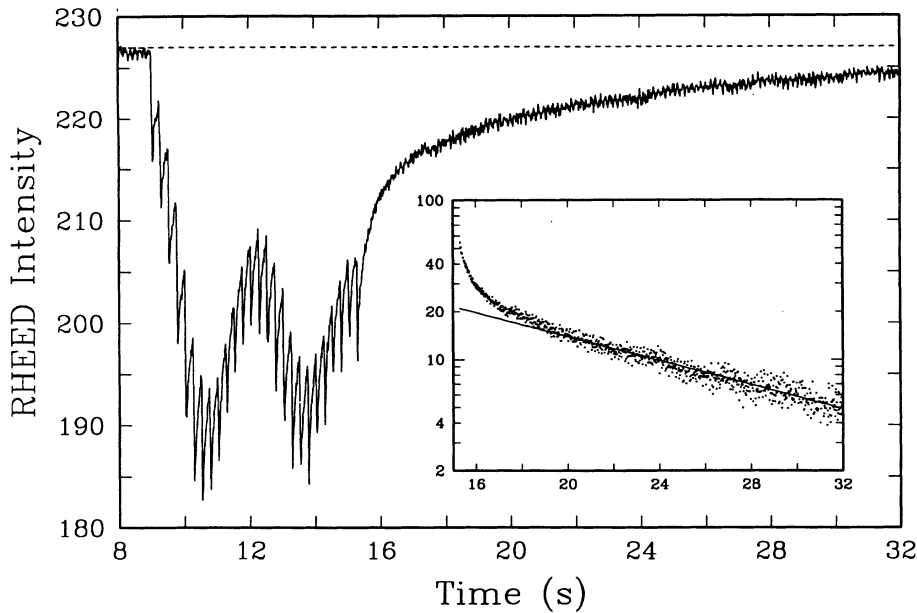


FIG. 11. RHEED intensity as a function of time for a YBCO film on (100) SrTiO₃ during the recovery period. Inset shows the RHEED intensity difference (base line minus signal) vs time in a semilog plot.

the film surface. Therefore, there is a reduction in the surface step density by migration of the surface adatoms to the flat terrace edges. With this model, a simple analysis of the time dependence of the RHEED intensity recovery after each interrupted growth cycle suggests that the surface smoothing at the growth front can be described by a surface diffusion constant $D_s \sim (l_D)^2/\tau$, where $\tau \approx 12$ s is the recovery time of the RHEED specular beam as estimated from Fig. 11 (inset) and $l_D \sim 1000$ Å, which yields $D_s \sim 10^{-12}$ cm²/s. This is consistent with the estimated value of the surface diffusion coefficient $D_s \sim 10^{-12}$ cm²/s inferred from the crossover from the screw-dislocation-mediated growth to the step-flow

growth mode [Fig. 4(d)] for the YBa₂Cu₃O_{7- δ} (1000–1500 Å thick) films grown on vicinal (100) SrTiO₃ substrates.¹⁴

Figure 12 shows two AFM micrographs and line scans for a ten-unit-cell YBCO epitaxial film deposited on a (100) SrTiO₃ substrate with the atomic oxygen enhanced growth-interruption technique at a background pressure of $P_0 \sim 10^{-3}$ Torr.

Critical temperature $T_c(R=0)$ of this 120 Å-thick film was measured to be 72 K with a metallic normal-state behavior. This film shows, over a scan area of $8 \mu\text{m} \times 8 \mu\text{m}$ [Fig. 12(a)], very little surface roughness and the corresponding line scan [Fig. 12(c)] reveals an average sur-

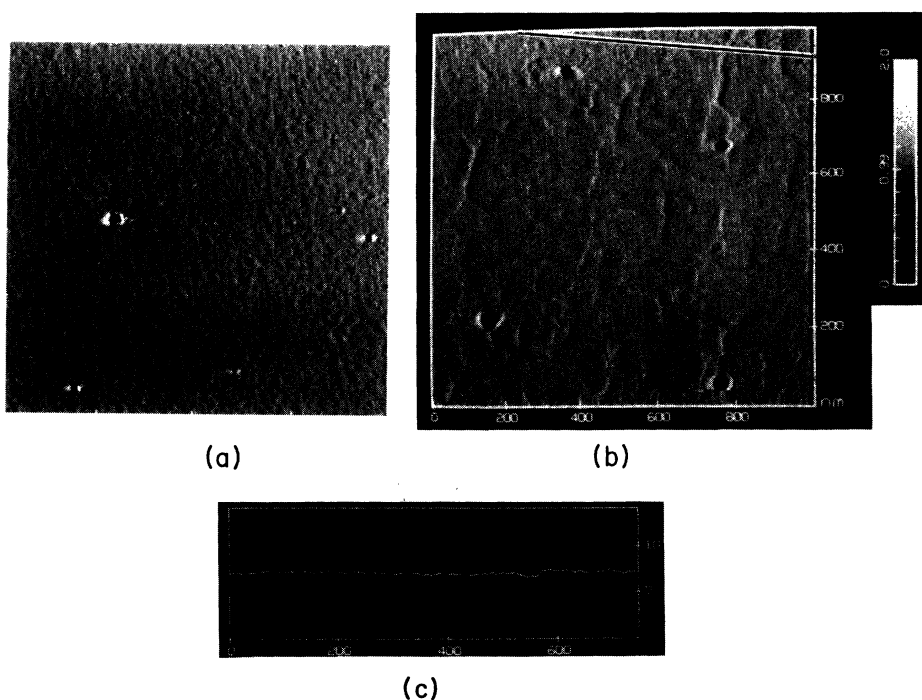


FIG. 12. (a) AFM micrograph ($8 \mu\text{m} \times 8 \mu\text{m}$) of a 120 Å-thick YBCO epitaxial film deposited on (100) SrTiO₃ using the atomic oxygen enhanced growth-interruption technique. Average surface roughness over the entire area is in the order of one uc (12 Å). (b) Enlarged area ($1 \mu\text{m} \times 1 \mu\text{m}$), and (c) a typical line scan. Representative height difference of the surface steps is ~ 7 Å. (All scales are in nm.)

face roughness of \sim one unit cell (12 \AA). Figure 12(b) shows an enlarged area ($1 \mu\text{m} \times 1 \mu\text{m}$) of this film. Over large areas, almost atomically smooth terraces with randomly distributed steps of, typically, $5\text{--}7 \text{ \AA}$ in height can be seen. Scanning over the entire sample ($0.5 \text{ cm} \times 1 \text{ cm}$ in size) results essentially in the same AFM image as those shown in Figs. 12(a)–12(c). With the assumption that there is no global gradient in film thickness, our AFM results imply that a smooth film surface over this area can be achieved. For thicker YBCO films (~ 20 unit cells) however, we only observe well-pronounced RHEED oscillations up to a total film thickness of $\sim 14\text{--}16$ uc deposition. The AFM picture of this 200-\AA -thick film shows a substantial surface roughening and randomly distributed island with multiple unit-cell step heights. Multiple nucleation sites together with a substantial increase in the interface width suggest a crossover from 2D nucleation to 3D film growth (Fig. 13).

On the other hand, a 10 uc YBCO film deposited without the aid of atomic oxygen is not stable under the ambient pressure of $P_0 \sim 2 \text{ mTorr O}_2$. The background pressure P_0 has to be increased to $\sim 8 \text{ mTorr}$ in order to get a stable film. Films prepared under this background pressure are insulating and show an increased surface roughness [Figs. 14(a) and 14(b)]. By comparing Figs. 12 and 14, it is evident that YBCO films prepared without the aid of atomic oxygen contain more island growth features with a typical step height of one unit cell (12 \AA) than similar thick YBCO films prepared with the use of atomic oxygen. It should be pointed out that a cuprate film (such as YBCO) deposited on a SrTiO_3 substrate can be strained and relatively dislocation free during its initial stage of epitaxy. Beyond the so-called critical thickness h_c , the strain at the interface is relaxed through the introduction of misfit dislocations resulting in a rough film surface. A rough estimate¹⁸ of h_c for an epitaxial

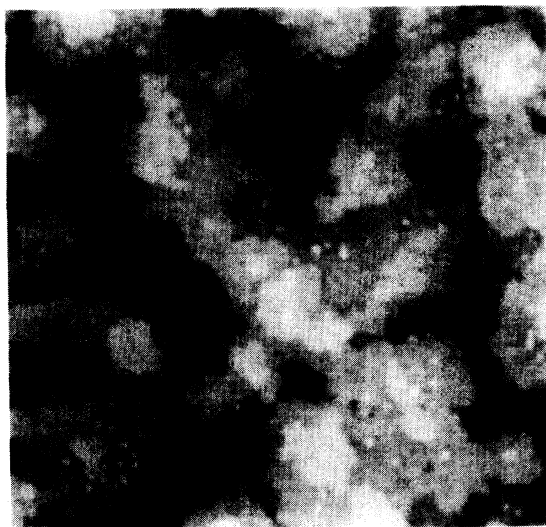
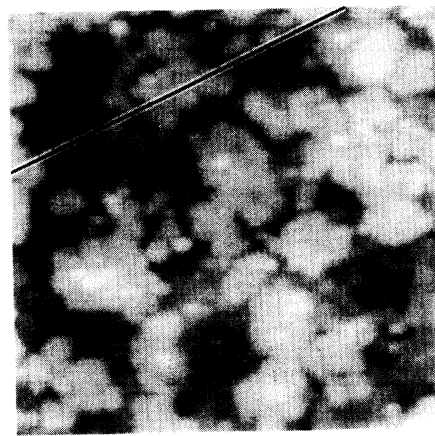


FIG. 13. AFM picture ($1.5 \mu\text{m} \times 1.5 \mu\text{m}$) of a 200 \AA -thick YBCO film grown with the atomic oxygen enhanced growth-interruption technique. Film shows a starting island growth mode along with the development of multiple nucleation sites. Step height between two adjacent terraces is 12 \AA .



(a)



(b)

FIG. 14. (a) AFM micrograph ($1.4 \mu\text{m} \times 1.4 \mu\text{m}$) of a 120 \AA -thick YBCO film deposited without the aid of atomic oxygen at $P_0 = 8 \text{ mTorr O}_2$. (b) Surface step height difference is 12 \AA indicated by arrows. (All scales are in nm.)

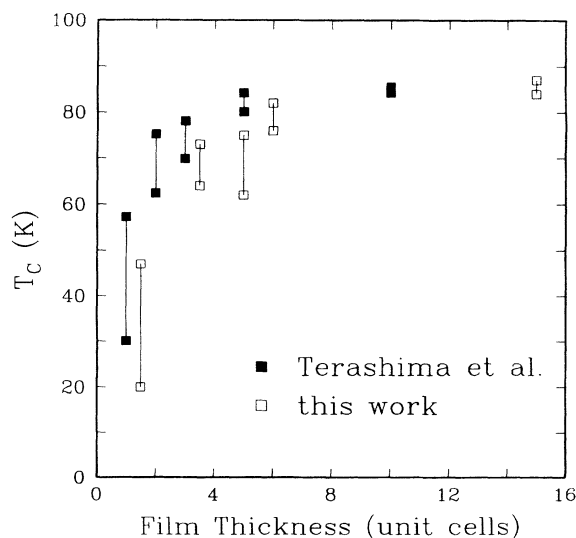


FIG. 15. T_c as a function of film thickness in units of unit cells, for YBCO epitaxial films deposited in (100) SrTiO_3 substrates with a six-uc-thick PBCO buffer layer (\square). For a given film thickness, the higher T_c value represents the midpoint of the resistive transition. The lower T_c value is the $R = 0$ transition temperature. For comparison, results by Terashima *et al.* (Ref. 1) are also shown in the figure (\blacksquare).

YBCO film on (100) SrTiO₃ suggests $h_c \sim 83 \text{ \AA}$ (\sim seven-uc thick for *c*-axis-oriented films) which is in reasonably good agreement with the values of h_c inferred experimentally from measurements such as STM surface imaging¹⁹ ($h_c \sim 8\text{--}16$ uc), and inclined direction channeling²⁰ ($h_c < 11$ uc). The results of this study, indeed, show that the surface roughness of films with thickness larger than 200 \AA (~ 17 -uc thick) are characteristically rougher (surface roughness $\sim 50 \text{ \AA}$ corresponding to four uc) than their thinner counterparts. The role of atomic oxygen is probably to lower the oxygen partial pressure and the substrate temperature required for stabilizing the high- T_c YBCO phase during epitaxial deposition and enhanced surface oxidation.

The epitaxial YBCO thin films deposited on the (100) SrTiO₃ substrate with a 6-uc PBCO buffer layer all exhibit a metallic normal-state behavior, and a systematic variation of T_c as a function of the YBCO film thickness (Fig. 15). The variation of T_c with the number of unit cells resembles that obtained by Terashima *et al.*¹ using reactive *e*-beam vapor deposition MBE and ozone as oxidant.

In summary, the growth mode of epitaxial cuprate films on a given substrate [such as atomically flat and

smooth (100) SrTiO₃] depends very much on the details of the competition between various thermodynamic and kinetic factors. In terms of surface energy, although *c*-axis-oriented two-dimensional growth is the thermodynamically preferred growth mode of YBa₂Cu₃O_{7- δ} , kinetically it is a rather inefficient process. However, one can manipulate the growth parameters to make sure that the atomistic surface mobility is high enough to support such a growth mode. The results of this study indicate that the use of an atomic oxygen ambient condition and the technique of surface self-smoothing helps to promote *c*-axis-oriented 2D growth of large area uc smooth superconducting YBCO films. The combined use of a relatively high substrate temperature T_s , and low deposition flux rate is consistent with the need for a low supersaturation at the substrate surface in order to favor two-dimensional layer growth.

ACKNOWLEDGMENTS

The authors wish to thank G. Trafas for technical assistance, A. Gupta, and Thomas Jung for useful discussions.

- ¹T. Terashima, Y. Bando, K. Lijima, K. Yamamoto, K. Hirata, K. Hayashi, K. Kamigaki, and H. Terauchi, *Phys. Rev. Lett.* **65**, 2684 (1990); T. Terashima, K. Shimura, Y. Bando, Y. Matsuda, A. Fujiyama, and S. Komiyama, *ibid.* **67**, 1362 (1991).
- ²N. Chandrasekhar, V. S. Achutharaman, V. Agrawal, and A. M. Goldman, *Phys. Rev. B* **46**, 8565 (1992); see also N. Chandrasekhar, V. S. Achutharaman, and A. M. Goldman (unpublished).
- ³Xiang-Yang Zheng, Douglas H. Lowndes, Shen Zhu, J. D. Budai, and R. J. Watmack, *Phys. Rev. B* **45**, 7584 (1992).
- ⁴S. J. Pennycook, M. F. Chisholm, D. E. Jesson, R. Feenstra, S. Zhu, X. Y. Zheng, and D. J. Lowndes, *Physica C* **202**, 1 (1992), and references therein.
- ⁵M. Y. Chern, A. Gupta, and B. W. Hussey, *Appl. Phys. Lett.* **60**, 3045 (1992).
- ⁶J. N. Eckstein, I. Bozovic, M. E. Klausmeier-Brown, G. F. Virshup, and K. S. Ralls, *Mater. Res. Bull.* **XVII**, 27 (1992), and references therein.
- ⁷T. Frey, C. C. Chi, C. C. Tsuei, T. Shaw, and G. Trafas, in *Layered Superconductors: Fabrication Properties and Applications*, MRS Symposia Proceedings No. 275 (Materials Research Society, Pittsburgh, 1992), p. 61.
- ⁸M. Kanai, T. Tomoji, and S. Kawai, *Jpn. J. Appl. Phys.* **31**, 331 (1992).
- ⁹*Reflection High-Energy Electron Diffraction and Reflection Electron Imaging from Surfaces*, edited by P. K. Larsen and

- P. J. Dobson (Plenum, London, 1989); J. H. Neave, B. A. Joyce, and P. J. Dobson, *Appl. Phys. A* **34**, 179 (1984); P. K. Larsen, P. J. Dobson, J. H. Neave, B. A. Joyce, B. Bölger, and J. Zhang, *Surf. Sci.* **169**, 176 (1986).
- ¹⁰B. A. Joyce, P. J. Dobson, and J. H. Neave, *Surf. Sci.* **174**, 1 (1986), and references therein.
- ¹¹J. H. Neave, B. A. Joyce, P. J. Dobson, and N. Norton, *Appl. Phys. A* **31**, 1 (1983).
- ¹²C. S. Lent and P. I. Cohen, *Surf. Sci.* **139**, 121 (1985).
- ¹³D. G. Schlom, D. Anselmetti, J. G. Bednorz, R. F. Broom, A. Catana, T. Frey, Ch. Gerber, H.-J. Guentherodt, H. P. Lang, and J. Mannhart, *Z. Phys. B* **86**, 163 (1992).
- ¹⁴D. G. Schlom, D. Anselmetti, J. G. Bednorz, Ch. Gerber, and J. Mannhart (unpublished).
- ¹⁵R. Borman and J. Nolting, *Appl. Phys. Lett.* **54**, 2148 (1989).
- ¹⁶R. H. Hammond and R. Bormann, *Physica C* **162-164**, 703 (1989).
- ¹⁷A. Tsukamoto, M. Hiratani, and S. Akamatsu, *Physica C* **181**, 369 (1991); Y. Yamamoto, B. M. Lairson, C. B. Eom, R. H. Hammond, J. C. Bravman, and T. H. Geballe, *Appl. Phys. Lett.* **57**, 1936 (1990).
- ¹⁸R. Gross, A. Gupta, A. Segmueller, and G. Koren (unpublished).
- ¹⁹X.-Y. Zheng, D. H. Lowndes, S. Zhu, J. D. Budai, and R. J. Warmack, *Phys. Rev. B* **45**, 7584 (1992).
- ²⁰X. X. Xi, J. Geerk, G. Linker, Q. Li, and O. Meyer, *Appl. Phys. Lett.* **54**, 2367 (1989).

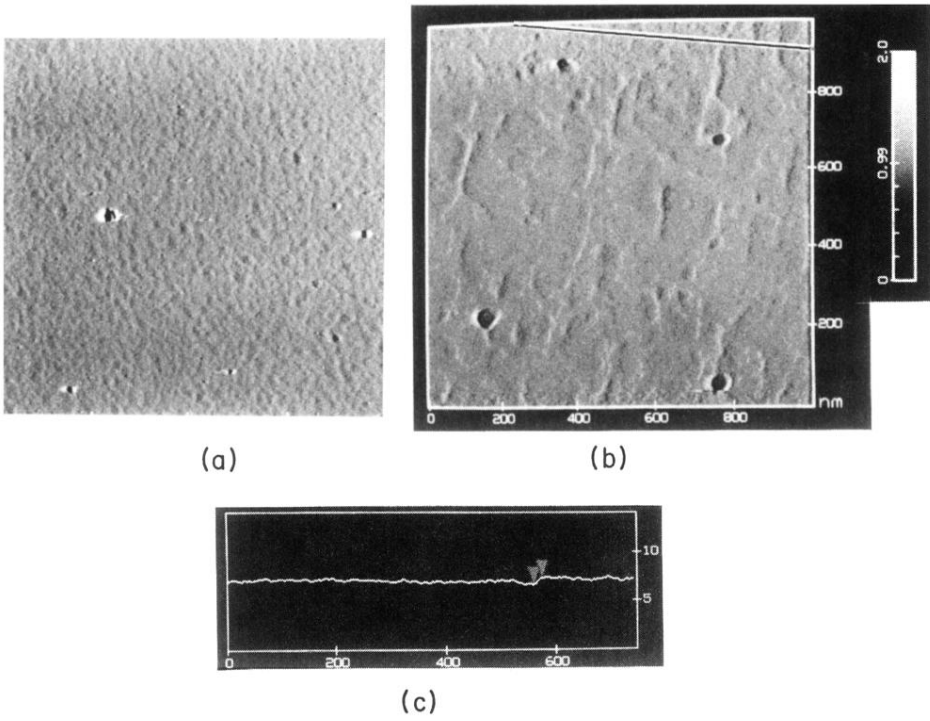


FIG. 12. (a) AFM micrograph ($8\ \mu\text{m} \times 8\ \mu\text{m}$) of a $120\ \text{\AA}$ -thick YBCO epitaxial film deposited on (100) SrTiO_3 using the atomic oxygen enhanced growth-interruption technique. Average surface roughness over the entire area is in the order of one uc ($12\ \text{\AA}$). (b) Enlarged area ($1\ \mu\text{m} \times 1\ \mu\text{m}$), and (c) a typical line scan. Representative height difference of the surface steps is $\sim 7\ \text{\AA}$. (All scales are in nm.)

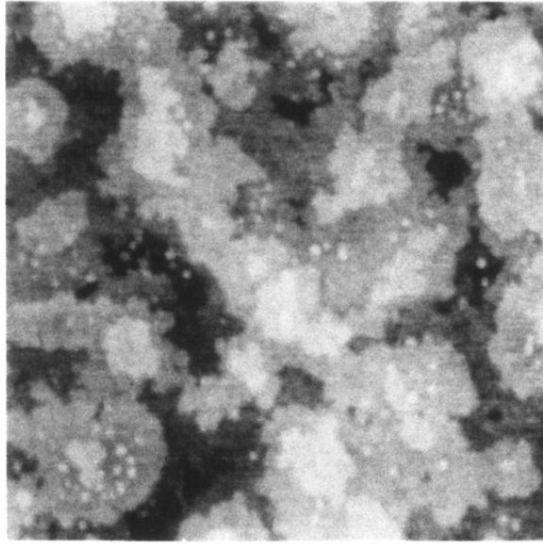
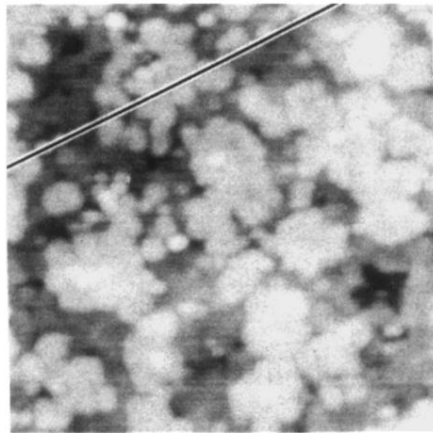
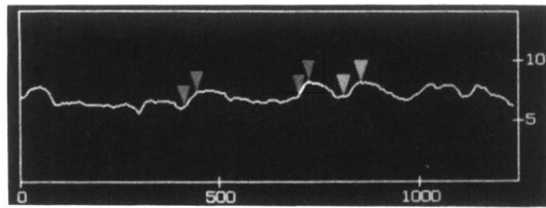


FIG. 13. AFM picture ($1.5\ \mu\text{m} \times 1.5\ \mu\text{m}$) of a $200\ \text{\AA}$ -thick YBCO film grown with the atomic oxygen enhanced growth-interruption technique. Film shows a starting island growth mode along with the development of multiple nucleation sites. Step height between two adjacent terraces is $12\ \text{\AA}$.

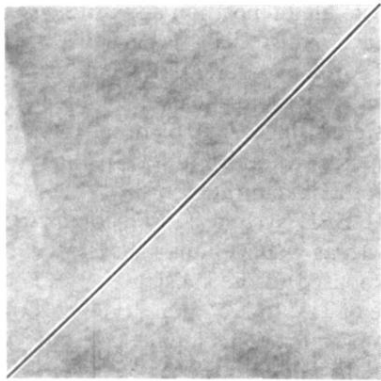


(a)

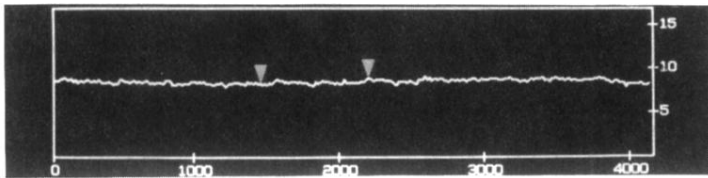


(b)

FIG. 14. (a) AFM micrograph ($1.4 \mu\text{m} \times 1.4 \mu\text{m}$) of a 120 Å-thick YBCO film deposited without the aid of atomic oxygen at $P_0 = 8 \text{ mTorr O}_2$. (b) Surface step height difference is 12 Å indicated by arrows. (All scales are in nm.)



(a)



(b)

FIG. 2. (a) AFM image ($3\ \mu\text{m} \times 3\ \mu\text{m}$) for a typical (100) SrTiO_3 substrate used in this study. (b) Typical line scan of the SrTiO_3 substrate with a corrugation of less than $5\ \text{\AA}$ over $4.2\ \mu\text{m}$. (Both vertical and horizontal scales are in nm.)

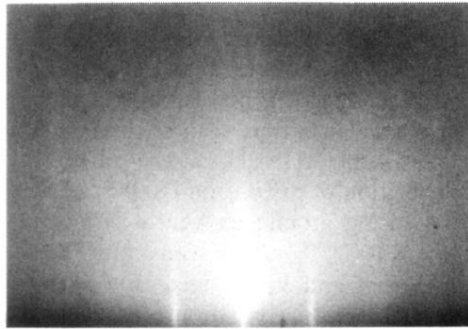
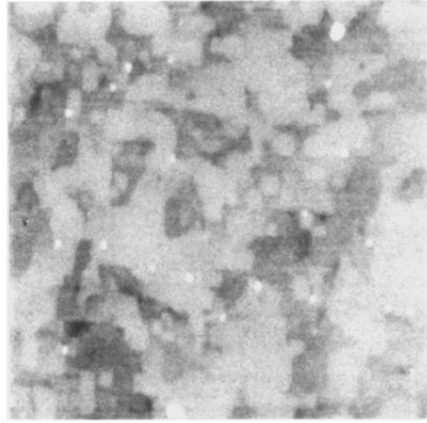
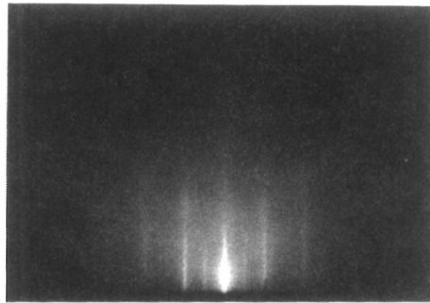


FIG. 3. RHEED patterns of the (100) SrTiO₃ along (100) substrate azimuth after homoepitaxial growth of a 18 monolayer (ML) buffer. ($T_s = 750^\circ\text{C}$, using atomic oxygen $P_0 \sim 10^{-4}$ Torr, beam energy 20 KeV.)



(a)



(b)

FIG. 7. (a) AFM image ($2\ \mu\text{m} \times 2\ \mu\text{m}$) of a $\sim 2000\ \text{\AA}$ -thick LSCO film. (b) RHEED patterns along the (100) azimuth of a $2000\ \text{\AA}$ -thick LSCO film at $T_s = 730^\circ\text{C}$. Beam energy $20\ \text{KeV}$.

Growth of unit-cell smooth films:
using RHEED-controlled
growth interruption technique

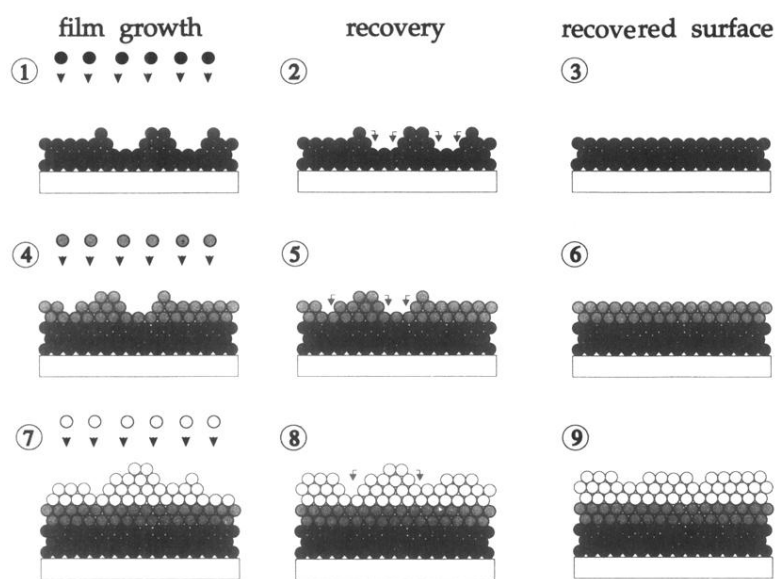


FIG. 9. Schematic diagram for the basic process of self-studying and self-substrate epitaxial growth. (Corresponding RHEED intensity oscillations are shown in Fig. 10.)